

Electron-phonon or hole superconductivity in MgB₂

J. E. Hirsch¹ and F. Marsiglio²

¹*Department of Physics, University of California, San Diego, La Jolla, California 92093-0319*

²*Department of Physics, University of Alberta, Edmonton, Alberta, Canada T6G 2J1*

(Received 27 February 2001; published 24 September 2001)

The BCS electron-phonon mechanism and the unconventional “hole mechanism” have been proposed as explanations for the high-temperature superconductivity observed in MgB₂. It is proposed that a critical test of which theory is correct is the dependence of T_c on hole doping: the hole mechanism predicts that T_c will drop rapidly to zero as holes are added, while the electron-phonon mechanism appears to predict increasing T_c for a substantial range of hole doping. Furthermore, the hole mechanism and electron-phonon mechanism differ qualitatively in their predictions of the effect on T_c of change in the $B-B$ distances. We discuss predictions of the hole mechanism for a variety of observables as a function of doping, emphasizing the expected differences and similarities with the electron-phonon explanation. The hole mechanism predicts coherence length and penetration depth to increase and decrease monotonically with hole doping, respectively.

DOI: 10.1103/PhysRevB.64.144523

PACS number(s): 74.20.-z, 74.70.-b

I. INTRODUCTION

Superconductivity at 40 K in MgB₂ was not predicted by theory. Soon after its discovery,¹ it was proposed that this finding is expected within two fundamentally different theoretical frameworks: the BCS electron-phonon theory^{2,3} and the theory of hole superconductivity.⁴ Both theories have claimed to be consistent with various experimental observations. The purpose of this paper is to expand on the predictions of the theory of hole superconductivity, and to make sharper the distinction between it and the electron-phonon theory *before* critical experiments are performed that can differentiate between both theories. It is generally easier to differentiate between theories by comparing their *predictions*, rather than their *postdictions*, of experimental observations; elaborate theoretical frameworks can often find consistent explanations even for the most unexpected observations.

It should be pointed out at the outset that the electron-phonon theories discussed in this paper do not include non-conventional versions such as proposed by Alexandrov⁵ and by Cappelluti *et al.*⁶ Those theories are proposed as replacements for the conventional electron-phonon theory when the electron-phonon coupling becomes strong⁵ and/or when nonadiabatic effects become important.^{5,6} It is possible that those theories will lead to different predictions than the conventional electron-phonon theory for MgB₂ and related compounds.

The electronic structure of MgB₂ is well established, as a variety of old⁷ as well as new^{2,3,8,9} calculations are in essential agreement. Approximately 30% of the density of states at the Fermi energy is due to planar boron $p_{x,y}$ states (σ bonds) that have little dispersion in the z direction, giving rise to nearly cylindrical hole Fermi surfaces of 2D character. The remaining 70% of the density of states originates in boron p_z states (π bonds) that are strongly hybridized with the Mg $s-p$ orbitals, have three-dimensional (3D) character and give rise to mostly electronlike Fermi surfaces. No d electrons exist in either Mg or B, so that magnetic and strong correlation mechanisms (generically called “big tent”

mechanisms¹⁰) proposed for the high- T_c cuprates, do not appear to be applicable.

Within the electron-phonon framework, two different explanations have been proposed, hereafter referred to as EP1 (Ref. 2) and EP2.³ Both explanations emphasize the importance of strong bonding of the boron atoms in giving rise to strong electron-phonon coupling, as well as the light ionic mass giving rise to a large prefactor in the BCS-Eliashberg expression for the transition temperature. They appear to differ in the relative contribution of the boron states. Whereas EP1 appears to suggest that contributions from all states are important, EP2 attributes superconductivity exclusively to the nearly full boron $p_{x,y}$ states. It is argued that the observation of a boron isotope effect¹¹ (isotope coefficient $\alpha = 0.29$) strongly favors electron-phonon mechanisms.^{2,3,11}

In contrast, within the theory of hole superconductivity^{12,13} the electron-phonon interaction is irrelevant, and instead superconductivity originates in undressing of hole carriers, driven by Coulomb interactions, in bands that are almost full. The superconducting condensation energy is kinetic, since paired carriers have lower effective mass than unpaired ones, and electron-hole symmetry breaking is central to the physics. In MgB₂, the fact that large parts of the Fermi surface are strongly holelike, together with the fact that the boron planes where the holes propagate are highly negatively charged, are proposed to be the essential factors giving rise to high T_c .⁴ The existence of an isotope effect is generically expected within this theory also,^{4,13} although its magnitude is difficult to calculate; a simple estimate yields⁴ a much larger isotope effect than observed experimentally in MgB₂ if the electron-phonon coupling suggested in Ref. 2 and 3 is used.

Both the electron-phonon theory and the hole theory predict that the superconducting state is s wave, which appears to be supported by tunneling¹⁴⁻¹⁷ as well as NMR (Ref. 18) measurements, and both theories are consistent with the observation of an isotope effect.¹¹ The theory of hole superconductivity *requires*⁴ that the conductivity in the normal state is holelike, which is consistent with recently reported Hall effect measurements;¹⁹ it also *requires*⁴ superconductivity to

disappear when the hole bands in MgB_2 become full, which is consistent with reported experimental results on $\text{Mg}_{1-x}\text{Al}_x\text{B}_2$.²⁰ Both of these facts apparently are consistent with electron-phonon theory, as discussed in EP2.³ On the other hand, the hole theory predicts that T_c should increase under pressure if the dominant effect is reduction of the B-B distances,⁴ while electron-phonon theory [EP1 (Ref. 2)] predicts that pressure generically should reduce T_c ; experiments show that hydrostatic pressure reduces T_c ,^{21,22} in apparent agreement with electron-phonon theory. We return to this point later in the paper.

A key prediction of both theories is the behavior of T_c upon hole doping, for example in the compound (not yet fabricated to our knowledge) $\text{Li}_x\text{Mg}_{1-x}\text{B}_2$. Here there is a clear opportunity for distinction between both theoretical frameworks. EP1 explicitly states that decreasing the Fermi level “may provide an additional contribution to λ ,” which suggests that T_c should increase upon hole doping. EP2 does not explicitly address this crucial point, but emphasizes the “substantial value of the Fermi level density of states,” even though “the hole density n_h is small.” Since the density of states increases with hole doping, both for the σ as well as for the π bands, for a very substantial range of hole doping, a reasonable inference within electron-phonon theory is that T_c should also increase with hole doping for a substantial range. Under the assumption that electron-phonon matrix elements, phonon frequencies and Coulomb pseudopotential do not change substantially, electron-phonon theory would predict that T_c should increase with hole doping in a range of about 2 eV below the Fermi level of MgB_2 (following the density of states increase), corresponding to ~ 0.36 holes added per B atom, and stay high (above the T_c of MgB_2) till about 4 eV below ϵ_F , corresponding to ~ 0.61 holes added per B atom. Instead, the theory of hole superconductivity predicts that T_c will rapidly drop when holes are added, becoming small or zero before the number of added holes per B atom reaches only 0.12. Comparison between these predictions of both theories will be discussed in detail in the next sections.

II. MODEL OF HOLE SUPERCONDUCTIVITY

Within the model of hole superconductivity, as well as within EP2, the bands that drive superconductivity are the nearly two-dimensional boron $p\sigma$ bands. Calculations for three-dimensional anisotropic band structures¹² have shown that a two-dimensional model reproduces the essential features, hence we will ignore the third dimension here for the calculations with the model of hole superconductivity. We will also approximate the nearly constant density of states of the hole $p\sigma$ bands by a constant, which has a negligible effect. The model is then defined by four parameters: U, K, W and D . D is the bandwidth, U the on-site Coulomb repulsion, W is proportional to the nearest-neighbor Coulomb repulsion, and K is proportional to the correlated hopping interaction Δt .

In the model of hole superconductivity, pairing of holes is driven by lowering of kinetic energy. First-principles calculations in small molecules have shown²³ that, in the param-

eter regime where interatomic distances and ionic charges are small, the hopping amplitude for a hole *increases* when another hole is at the site the first hole is hopping to or from. This quantum-mechanical effect occurs due to Coulomb interactions between electrons and between electrons and ions, with the ions *fixed* in their equilibrium positions. It gives rise to a difference in hopping amplitudes Δt that favors pairing of holes, and will drive the system superconducting if the Fermi level is close to the top of the band. Generally, an isotope effect also occurs, due to the modification of Δt due to ionic displacement; however, a value of the electron-phonon coupling much smaller than needed in the conventional BCS-Eliashberg theory to account for T_c will give rise to a substantial isotope effect in this theory;⁴ furthermore, the system will remain superconducting even in the limiting case when the ionic mass goes to infinity.

The BCS pairing interaction is given by $V_{kk'}$ $\equiv V(\epsilon_k, \epsilon_{k'})$, with

$$V(\epsilon, \epsilon') = U + 2\frac{K}{D}(\epsilon + \epsilon') + 4\frac{W}{D^2}\epsilon\epsilon'. \quad (1)$$

The critical temperature is determined by the equation

$$1 = 2KI_1 - WI_2 - UI_0 + (K^2 - WU)(I_0I_2 - I_1^2) \quad (2)$$

and the parameters Δ_m and c that define the energy-dependent gap

$$\Delta(\epsilon) = \Delta_m \left(-\frac{\epsilon}{D/2} + c \right) \quad (3)$$

by the equations

$$1 = K(I_1 + cI_0) - W(I_2 + cI_1), \quad (4a)$$

$$c = K(I_2 + cI_1) - U(I_1 + cI_0) \quad (4b)$$

with

$$I_l = \frac{1}{D} \int_{-D/2}^{D/2} d\epsilon \left(-\frac{\epsilon}{D/2} \right)^l \frac{1 - 2f(E(\epsilon))}{2E(\epsilon)} \quad (5a)$$

$$E(\epsilon) = \sqrt{(\epsilon - \mu)^2 + \Delta(\epsilon)^2} \quad (5b)$$

with f the Fermi function and μ the chemical potential. Finally, the hole density n_h is determined by the equation

$$n_h = 1 - \frac{2}{D} \int_{-D/2}^{D/2} d\epsilon (\epsilon - \mu) \frac{1 - 2f(E(\epsilon))}{2E(\epsilon)}. \quad (6)$$

III. CHOICE OF PARAMETERS

The density of states at the Fermi level of MgB_2 is estimated to be 0.75 states/eV, of which approximately 0.25 states/eV is ascribed to the B $p\sigma$ states.^{2,3} In a model with constant density of states and a single band, that would correspond to $D = 4$ eV. There are two $p\sigma$ bands that contribute to this density of states, approximately with 2/3 and 1/3 weight³ (heavy and light hole bands, respectively, in the nomenclature of An and Pickett). According to An and Pickett,

the equivalent two-dimensional flat bands have densities of states 0.18 states/eV and 0.07 states/eV, which would correspond to bandwidths $D_1=5.6$ eV, $D_2=14$ eV, respectively. The total number of holes in the B $p\sigma$ bands for MgB₂ is estimated to be $n_h=0.13$ /unit cell, of which approximately 0.09 and 0.044 holes are in the heavy and light hole bands, respectively. The total n_h per B atom in MgB₂ is approximately 0.067.

We will discuss elsewhere the results of our theory in the presence of two hole bands, which we do not expect will be qualitatively different.²⁴ Here, we will use a single “effective band” of bandwidth $D=5$ eV, Coulomb repulsion $U=5$ eV and nearest-neighbor repulsion $W=0$. As we will discuss in a later section, the model gives similar results for a wide range of parameters. For these parameters, we choose the value of K required to yield $T_c=40$ K for $n_h=0.067$, which is $K=2.97$ eV. As discussed elsewhere,⁴ we believe this value of K is reasonable for MgB₂, but emphasize that here K is a fitting parameter as we have not obtained it from a first-principles calculation.

IV. T_c VERSUS DOPING

As discussed in the introduction, no calculations of T_c versus hole doping with the electron-phonon model (EP1 or EP2) have yet been reported. It is possible that such calculations may indicate large changes in the phonon frequencies, electron-phonon matrix elements or Coulomb pseudopotential with doping. In the absence of other information, however, we will assume that all these quantities are constant with doping, and calculate T_c within the electron-phonon model by the modified McMillan formula,²

$$T_c = \frac{\langle \omega_{log} \rangle}{1.2} e^{-1.02 \frac{(1+\lambda)}{\lambda - \mu^* - \mu^* \lambda}} \quad (7)$$

with $\mu^*=0.1$ and $\langle \omega_{log} \rangle=700$ K,² and λ proportional to the density of states in the B $p\sigma$ band. Because the fractional contribution of the B $p\sigma$ bands to the total density of states is quite constant with doping (1/3), this calculation should predict the results of both electron-phonon models EP1 and EP2 under the assumption that electron-phonon matrix elements, phonon frequencies and μ^* do not change with doping.

Figure 1 shows the results of this calculation for the two models, as function of hole content in the $p\sigma$ bands per B atom, n_h . Note that n_h is approximately 1/3 of the total hole doping per unit cell, n_h^{tot} . The electron-phonon model predicts that T_c will continue to increase well beyond the point where the hole model predicts T_c will have vanished; the maximum T_c of 94 K occurs for $n_h=0.43$ per B atom, or total hole doping of MgB₂ of approximately $n_h^{tot} \sim 1.1$ holes per unit cell, corresponding to bringing the Fermi level down approximately 2.1 eV from its position in MgB₂. In contrast, the maximum T_c in the hole model of 49 K occurs for $n_h \sim 0.035$ per B atom, corresponding to *electron* doping of MgB₂ of approximately 0.03 electrons per B atom, or 0.09 electrons per unit cell.

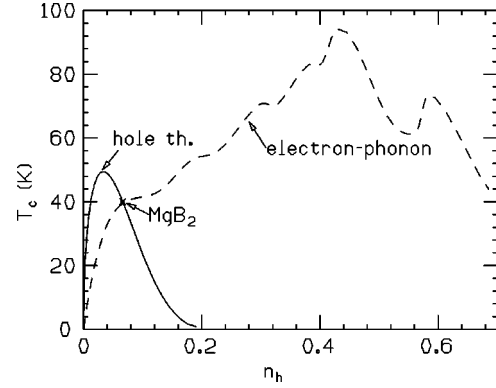


FIG. 1. Comparison of the predictions for variation of the critical temperature with hole doping in the model of hole superconductivity (full line) and the electron-phonon model (dashed line). Here and in the following figures, n_h is the average hole content per boron atom; the total hole doping per unit cell is approximately three times larger. The results for electron-phonon theory were obtained assuming constant electron-phonon matrix elements and phonon frequencies, and using the density of states values obtained in the band-structure calculation in Ref. 2.

As mentioned above, these results could be modified in the electron-phonon model if there are substantial changes in some or all phonon frequencies, electron-phonon matrix elements, or Coulomb pseudopotential. In the hole model, some modification may be expected if the contribution of the two B $p\sigma$ bands is taken into account separately. In particular, assuming it is the heavy hole band that dominates T_c , T_c would go to zero in an even narrower range of hole doping than indicated by Fig. 1. Despite these caveats, we believe the qualitative difference in the behavior predicted by the hole model and by the electron-phonon models depicted in Fig. 1 is robust.

V. PRESSURE DEPENDENCE OF T_c

In the hole model, a decrease in the B-B intraplane distances should strongly increase T_c . So far, only observations of changes in T_c under hydrostatic pressure on polycrystalline samples have been reported^{21,22} that indicate that such pressure decreases T_c . We believe that hydrostatic pressure is likely to affect much more strongly the lattice spacing in the c direction than the planar lattice spacings, due to the stiffness of the $p\sigma$ bonds. Furthermore, it is possible that substantial charge transfer occurs between different bands when pressure is applied. For example, in many high- T_c cuprates the hole concentration in the planes is increased by approximately 10% when 1 GPa hydrostatic pressure is applied.²⁵ According to Fig. 1, a 10% increase in hole content from MgB₂ leads to a decrease in T_c of 3 K; the reported observation of a decrease in T_c by 1.6 K (Ref. 21) could hence be accounted for by such an increase in the B $p\sigma$ orbitals hole content together with a small decrease in the B-B distances. Hence the observation is not necessarily inconsistent with our model, as is also emphasized in Ref. 21.

Here we consider the effect on T_c of a decrease in the B-B intraplane distances. The intrinsic effect of changing lattice

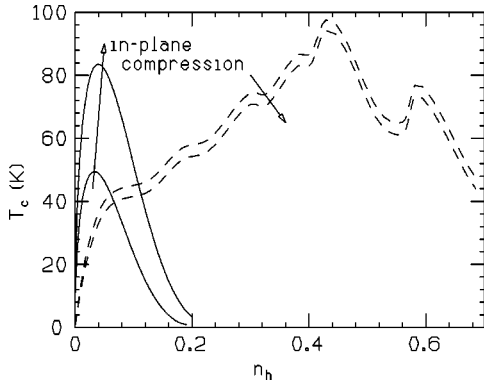


FIG. 2. Comparison of the predictions for variation of the critical temperature with in-plane B-B distance in the model of hole superconductivity (full lines) and the electron-phonon model (dashed lines). The bandwidth and density of states are assumed to change by 5%. Again, the results for electron-phonon theory were obtained assuming constant electron-phonon matrix elements and phonon frequencies under compression.

spacing in the c direction should be much smaller within our model.²⁶ In the electron-phonon model, we assume the dominant effect will be to decrease the density of states. In the hole model, we assume the effect is to increase the bandwidth (i.e., decrease the density of states) and increase the interaction parameter K that depends on overlap matrix elements as the bandwidth does, by the same fraction.

Figure 2 shows the changes expected under a 5% change in these parameters, achieved by either physical or chemical pressure. In the electron-phonon model (again assuming no change in phonon frequencies, electron-phonon matrix elements, and μ^*), a small decrease in T_c results. In the hole model, a strong increase in the critical temperature for all hole dopings results. By performing such experiments and monitoring the changes in lattice constants and in carrier concentration (e.g., through Hall measurements) we hope it will be possible to decide which of the two qualitatively different behaviors shown in Fig. 2 takes place in this class of materials.

VI. OTHER RESULTS FOR THE MODEL OF HOLE SUPERCONDUCTIVITY

We next discuss other results for our model for a single band with constant density of states, in the range of parameters that may be appropriate for this class of materials. Figure 3 illustrates the effect of changing Coulomb interaction parameters in the model, always choosing the parameter K so as to yield the observed value $T_c \sim 40$ K for $n_h = 0.065$. It can be seen that the behavior of T_c versus doping is quite insensitive to large variations in the Coulomb interactions. On increasing the nearest-neighbor repulsion the range of hole dopings where T_c is nonzero increases somewhat, and on increasing the on-site Coulomb interaction that range decreases. If the Coulomb repulsion appropriate for MgB_2 is larger than 5 eV, the maximum T_c obtained by electron doping could be larger than 50 K, as seen in Fig. 3.

Figure 4 illustrates the effect on T_c of changing the band-

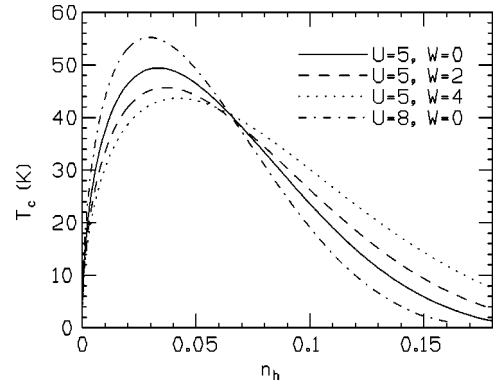


FIG. 3. T_c versus hole concentration for bandwidth $D = 5$ eV and various values of Coulomb interaction parameters, given in the figure in eV. The values for the correlated hopping parameter used for the four cases shown are in eV, $K = 2.97, 4.115, 5.135, 4.134$, respectively, in the order given in the figure label.

width, i.e., the density of states. It can be seen that the effect is again remarkably small, with a reduction in the bandwidth leading to a small decrease in the range of hole concentration where T_c is nonzero.

We next calculate other observables for the parameters of Fig. 4. Figure 5 shows the behavior of the coherence length ξ_o , defined as the average size of the pair wave function, with hole doping. The formulas to evaluate this quantity for the model under consideration here are given in Ref. 27. The coherence length is found to be almost independent of the values of the Coulomb interactions, but it depends strongly on the bandwidth, as seen in the different curves in Fig. 5: as the bandwidth decreases, the coherence length decreases. The coherence length in Fig. 5 is given in units of lattice spacings in an effective square lattice; to transform to physical units for MgB_2 ($a = 3.14$ Å), a lattice spacing $a_{eff} = 2.22$ Å should be used. For hole concentration $n_h = 0.065$, the result obtained with $D = 2.5$ eV is close to the observed experimental value, $\xi_o = 45$ Å.^{28,29} Instead, for $D = 5$ eV we obtain a coherence length of $\xi_o = 83$ Å, larger

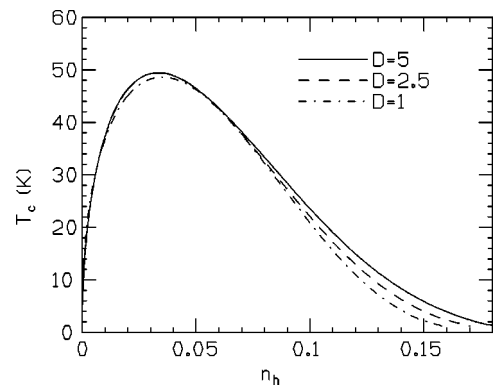


FIG. 4. T_c versus hole concentration for on-site Coulomb repulsion $U = 5$ eV, $W = 0$, and various values of the bandwidth D , given in the figure in eV. The values for the correlated hopping parameter used for the three cases shown are in eV, $K = 2.97, 2.496, 1.963$, respectively, in the order given in the figure label.

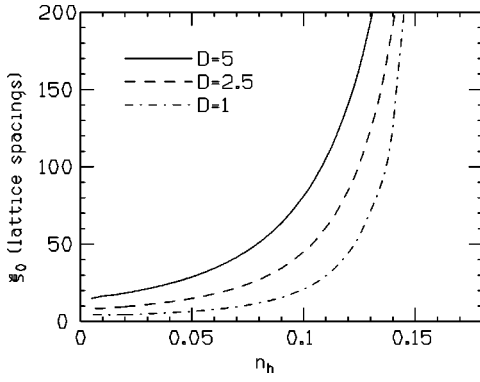


FIG. 5. Coherence length (in units of the lattice spacing) versus doping for the three sets of parameters of Fig. 4. A lattice spacing corresponds to 2.2 Å.

than seen experimentally. However, our calculated value corresponds to the in-plane coherence length which is not necessarily the same as that measured in a polycrystalline sample. As seen in Fig. 5, the coherence length is predicted to increase monotonically with hole doping.

Similarly, Fig. 6 shows the behavior of the in-plane London penetration depth λ_L , assuming the clean limit:

$$\lambda_L = 4638[d(\text{Å})]^{1/2} \frac{1}{T_a(\text{meV})^{1/2}} \quad (8)$$

with d the distance between boron planes, $d = 3.52$ Å and T_a the average in-plane kinetic energy per boron atom. The estimated value for MgB₂ is $\lambda_L = 1400$ Å,²⁸ which is close to the value given in Fig. 6 for $D = 2.5$ eV and $n_h = 0.065$, $\lambda_L = 1344$ Å. For $D = 5$ eV we obtain a smaller value than seen experimentally. The penetration depth is predicted to decrease monotonically with hole doping. In conjunction with the increasing coherence length, this implies that the Ginzburg-Landau parameter $\kappa = \lambda_L / \xi_0$ will rapidly decrease with hole doping, which could eventually lead to a crossover from type-II to type-I behavior for high hole doping. However, this is likely to be prevented by disorder, that would cause an increase in the penetration depth from its clean limit value.

The gap versus hole concentration follows closely the behavior of the critical temperature. This is shown in Fig. 7. In

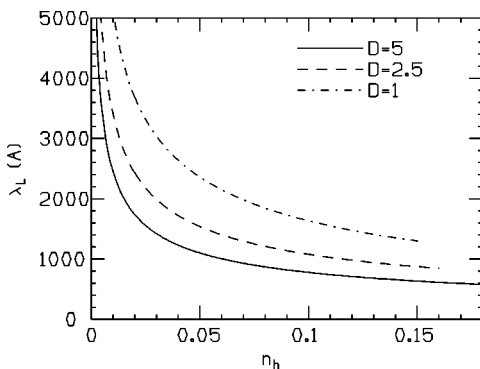


FIG. 6. London penetration depth versus doping for the three sets of parameters of Fig. 4.

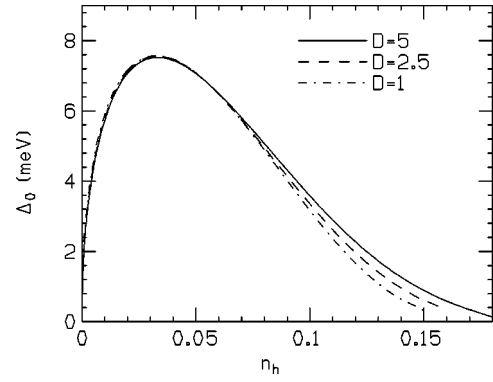


FIG. 7. Gap versus hole doping for the three sets of parameters given in Fig. 4.

contrast to high- T_c oxides, we do not find a substantial increase in the gap ratio in the underdoped regime, because the parameters here correspond to a weak-coupling regime. In Fig. 8 we show the hole concentration dependence of the specific heat jump at T_c , which agrees with the BCS weak-coupling value 1.43 for high hole concentrations and becomes larger for low hole concentrations, particularly as the bandwidth becomes smaller.

The temperature dependence of various quantities obtained from our model also follows closely the BCS weak-coupling behavior. As an example we show results for the gap ratio and the specific heat for one parameter set in Fig. 9. Experimental results for specific heat of MgB₂ show a clear specific-heat jump at the transition with value close to the expected BCS value.³⁰

Finally Fig. 10 shows tunneling characteristics for one set of parameters and hole doping appropriate to MgB₂. Again the behavior resembles the weak-coupling BCS results for an s -wave gap, except for the existence of asymmetry. As emphasized elsewhere,¹² an asymmetry of universal sign occurs for this model, with a larger peak for a negatively biased sample. The case of Fig. 10 corresponds to the smallest bandwidth considered; for larger bandwidth the magnitude of tunneling asymmetry decreases.

VII. CONCLUSIONS

The growing number of experimental results on MgB₂ suggests that superconductivity in these materials is more

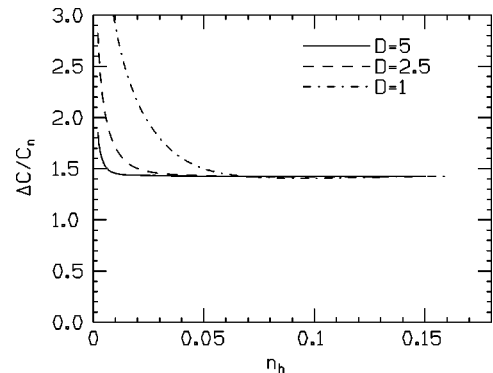


FIG. 8. Specific heat jump versus doping for the three sets of parameters of Fig. 4.

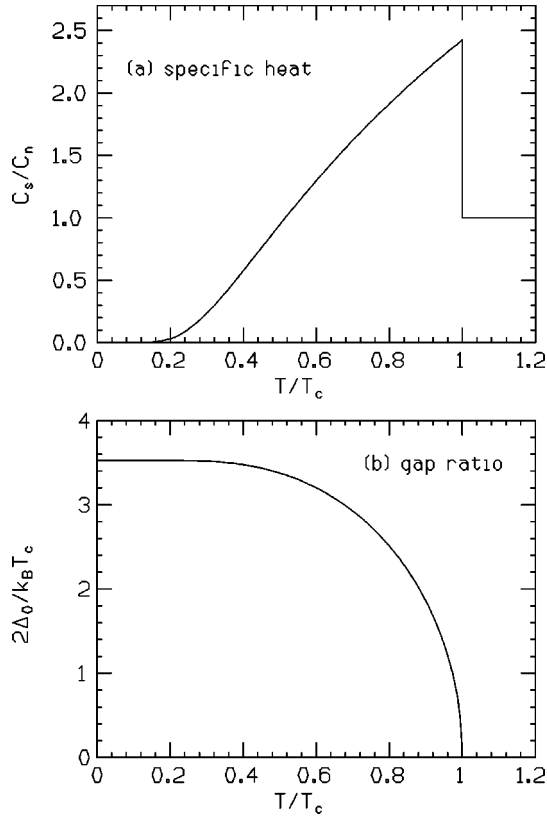


FIG. 9. Temperature dependence of specific heat (a) and of energy gap (b) for the parameters of Fig. 1 and doping $n_h=0.065$.

akin to conventional superconductivity than it is to high-temperature superconductivity in the cuprates. Thus it is natural that a consensus is growing that MgB_2 is describable within the conventional BCS-electron-phonon framework. However, we have proposed in Ref. 4 that instead MgB_2 should be described by the model of hole superconductivity, just as the high- T_c cuprates.¹² The common elements in the two classes of materials are that conduction is dominated by carriers in nearly filled bands, i.e., of holelike character, and that the carriers that drive superconductivity propagate in

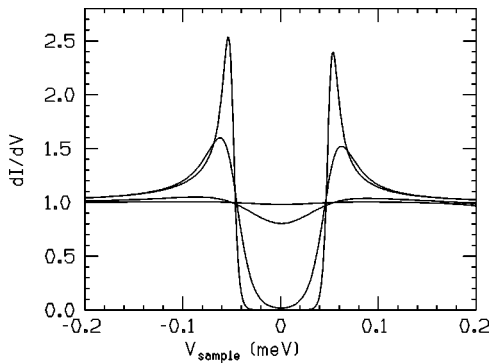


FIG. 10. Tunneling characteristics for the parameters of Fig. 4 with $D=1$ eV, doping $n_h=0.065$, and temperatures $T/T_c = 0.99, 0.9, 0.3, 0.1$. Note the higher peak when the sample is negatively biased. For larger bandwidths the magnitude of the asymmetry decreases.

conducting substructures that are highly negatively charged (planes). Differences in the behavior of the two classes of materials arise within the model of hole superconductivity from the fact that they are in different parameter regimes: the high- T_c cuprates are in a substantially stronger coupling regime (as indicated by the shorter coherence lengths), particularly for low hole doping.³¹ Compelling aspects of the theory of hole superconductivity are that it can describe superconductivity in a wide range of coupling regimes, and that it could be a universal theory of superconductivity for all materials.¹³

In the weak-coupling regime, the predictions of the model of hole superconductivity are similar to those of conventional BCS theory, and hence to the predictions of weak-coupling electron-phonon BCS theory. Hence experimental evidence for BCS behavior in, e.g., temperature dependence of the gap,¹⁵ or in tunneling characteristics,¹⁴⁻¹⁷ should not be taken to favor the electron-phonon model over the model of hole superconductivity. The isotope effect, conventionally assumed to favor the electron-phonon model, is also expected within the model of hole superconductivity,¹³ and hence should also not be used to differentiate between both models. An Eliashberg analysis of fine structure in tunneling characteristics above the gap energy, that traditionally has been assumed to be the strongest proof for the electron-phonon mechanism, has not yet been performed for this material.

Here we have focused on two properties that show a clear difference in the electron-phonon and the hole model. One is the hole doping dependence of the critical temperature, which the hole model predicts to be much stronger than the electron-phonon model. These experiments have not yet been performed, and once experimental results become available it will be possible to ascertain which of both models is favored. Of course it is possible that even if experiments show that superconductivity is rapidly suppressed with hole doping, as the hole model predicts, electron-phonon theory may also account for it if a rapid decrease of electron-phonon matrix elements or of the relevant phonon frequencies with hole doping is postulated to occur, or if a rapid increase in the Coulomb pseudopotential μ^* with hole doping is postulated to occur. If so, electron-phonon theory (e.g., in its EP2 version) and the hole theory will become increasingly indistinguishable.

The other property that shows a clear difference in the electron-phonon models and the hole model is the pressure dependence of T_c for uniaxial pressure that modifies the intraplane B-B distances: the hole model predicts a strong increase in T_c , and the electron-phonon model a (weaker) decrease in T_c . Again, once experimental results become available it will be possible to decide which model is favored. However, here again it is possible that even if experiments show that T_c is strongly enhanced by reduction of the intraplane B-B distance, electron-phonon theory could account for it if a concomitant increase of electron-phonon matrix elements or of the relevant phonon frequencies is postulated to occur or a concomitant decrease of Coulomb pseudopotential is postulated to occur.

Assuming experimental results will show a rapid decrease

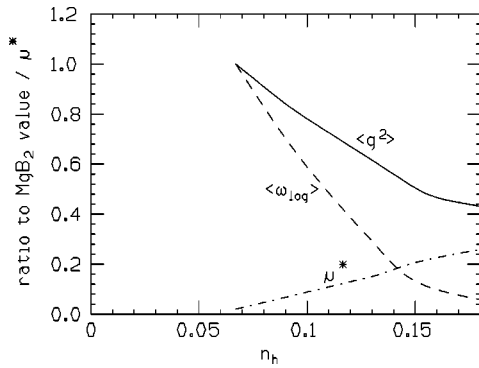


FIG. 11. Variation of the electron-phonon matrix element $\langle g^2 \rangle$ (solid line), the average phonon frequency $\langle \omega_{log} \rangle$ (dashed line), and the Coulomb pseudopotential μ^* (dash-dotted line) required, if T_c is given by the electron-phonon model Eq. (7), to yield the rapid drop of T_c with hole doping predicted by the model of hole superconductivity. In each case it is assumed that the other parameters are fixed at their values for MgB₂. Density of states values obtained from Ref. 2 are used.

of T_c with hole doping as predicted by our theory, it is interesting to examine how the parameters in electron-phonon models would have to change to account for such a drop, given the band-structure results for the density of states shown in Fig. 1. Figure 11 shows three possible scenarios: (i) the behavior required for the average of the square of the electron-phonon matrix element $\langle g^2 \rangle$ versus hole doping of the B atoms, assuming the phonon frequencies of the relevant phonons and the Coulomb pseudopotential μ^* stay constant; (ii) the behavior required for the phonon frequencies of the relevant phonons $\langle \omega_{log} \rangle$, assuming the electron-phonon matrix elements and μ^* stay constant, and (iii) the behavior required for the Coulomb pseudopotential μ^* , assuming the electron-phonon matrix elements and phonon frequencies of the relevant phonons stay constant. It can be seen that in all cases a rather rapid variation of parameters with hole doping is required. Of course a suitable combination of decrease in electron-phonon matrix elements and phonon frequencies and increase in μ^* could also account for such behavior. It should be stressed that such rapid variations of electron-phonon matrix elements, phonon frequencies, and/or μ^* with hole doping have so far not been predicted by the electron-phonon models.^{2,3}

The range of hole doping where superconductivity occurs in our model is not strongly dependent on the parameters in the model for a wide range of parameters, as was shown in Figs. 3 and 4. Hence the prediction that superconductivity should only occur in a narrow range of doping around MgB₂

is a strong prediction of the model. If the band-structure results for the position of the Fermi level are correct, it implies that MgB₂ is somewhat overdoped in our model, and hence doping with electrons should increase T_c . This is in apparent contradiction with experimental results for Mg_{1-x}Al_xB₂.²⁰ Possible explanations for the discrepancy may be problems with sample quality, or that the lattice constants change with increasing Al content.

We have also examined here the predictions of the model of hole superconductivity for various observables in a range of parameters that appears to be appropriate for MgB₂. Because this is a weak-coupling regime, most properties are found to be very close to conventional BCS behavior. If the appropriate bandwidth is rather small the universal asymmetry in tunneling predicted by the theory becomes of appreciable magnitude. We found the penetration depth decreasing monotonically with hole doping (assuming the clean limit), which is the same qualitative behavior seen in high- T_c cuprates.³² The coherence length was found to increase monotonically with hole doping, which is also seen in high- T_c materials. If experiments confirm these predictions they will support the proposed commonality in the physics of superconductivity in the cuprates and in MgB₂-derived compounds. Given this behavior, in the absence of disorder a crossover from type-II to type-I behavior with hole doping should eventually occur. While disorder is likely to prevent this in alloys, we expect that if similar stoichiometric compounds with larger hole content than MgB₂ are found they will have a smaller Ginzburg-Landau parameter κ than MgB₂ ($\kappa \sim 26$),²⁸ and possibly even be type I.

Superconducting properties as function of hole doping have not yet been discussed within electron-phonon models. We note, however, that the strong increase of density of states expected with hole doping suggests that electron-phonon theory may describe a crossover to a stronger coupling regime with hole doping, i.e., decreasing coherence length and increasing penetration depth. We stress that this would be in qualitative disagreement with our predictions.

In future work we will examine the predictions of our model taking into account the presence of two different hole bands, and the effect of the anisotropic band structure, in order to calculate observables in different directions which will be of interest once experimental results in single crystals become available.

ACKNOWLEDGMENTS

F.M. was supported by the Natural Sciences and Engineering Research Council (NSERC) of Canada and the Canadian Institute for Advanced Research.

¹J. Akimitsu, Symposium on Transition Metal Oxides, Sendai, January 2001; J. Nagamatsu *et al.*, Nature (London) **410**, 63 (2001).

²J. Kortus, I.I. Mazin, K.D. Belashchenko, V.P. Antropov, and L.L. Boyer, Phys. Rev. Lett. **86**, 4656 (2001).

³J.M. An and W.E. Pickett, Phys. Rev. Lett. **86**, 4366 (2001).

⁴J.E. Hirsch, cond-mat/0102115 (unpublished); Phys. Lett. A **282**, 392 (2001).

⁵A.S. Alexandrov, Physica C **341-348**, 107 (2000), and references therein.

⁶E. Cappelluti, C. Grimaldi, L. Pietronero, and S. Strassler, Int. J. Mod. Phys. B **14**, 2938 (2000), and references therein.

- ⁷D.R. Armstrong and P.G. Perkins, J. Chem. Soc., Faraday Trans. 2 **75**, 12 (1979).
- ⁸K.D. Belashchenko, M. van Schilfgaarde, and V.P. Antropov, cond-mat/0102290 (unpublished).
- ⁹G. Satta *et al.*, cond-mat/0102338 (unpublished).
- ¹⁰P.W. Anderson, Physica C **341-348**, 9 (2000); in *High Temperature Superconductivity*, edited by S.E. Barnes, J. Ashkenazi J.L. Cohn, and F. Zuo, AIP Conf. Proc. **483**, AIP, Woodbury, NY, 3 (1999).
- ¹¹S.L. Bud'ko, G. Lapertot, C. Petrovic, C.E. Cunningham, N. Anderson, and P.C. Canfield, Phys. Rev. Lett. **86**, 1877 (2001).
- ¹²J.E. Hirsch and F. Marsiglio, Phys. Rev. B **39**, 11 515 (1989); Physica C **162-164**, 591 (1989); Phys. Rev. B **62**, 15 131 (2000), and references therein.
- ¹³J.E. Hirsch, Physica C **158**, 326 (1989); Phys. Lett. A **138**, 83 (1989); Physica C **341-348**, 213 (2000), and references therein; Phys. Rev. B **62**, 14 487 (2000); **62**, 14 498 (2000); cond-mat/0102136 (unpublished), and references therein.
- ¹⁴G. Rubio-Bollinger, H. Suderov, and S. Vieira, Phys. Rev. Lett. **86**, 5582 (2001).
- ¹⁵G. Karapetrov, M. Iavarone, W.K. Kwok, G.W. Crabtree, and D.G. Hinks, Phys. Rev. Lett. **86**, 4374 (2001).
- ¹⁶A. Sharoni, I. Felner, and O. Millo, Phys. Rev. B **63**, 220504 (2001).
- ¹⁷H. Schmidt, J.F. Zasadzinski, K.E. Gray, and D.G. Hinks, Phys. Rev. B **63**, 220504 (2001).
- ¹⁸H. Kotegawa *et al.*, cond-mat/0102334 (unpublished).
- ¹⁹W.N. Kang *et al.*, cond-mat/0102313 (unpublished).
- ²⁰J.S. Slusky *et al.*, Nature (London) **410**, 343 (2001).
- ²¹B. Lorenz, R.L. Meng, and C.W. Chu, Phys. Rev. B **64**, 012507 (2001).
- ²²B. Maple *et al.* (private communication).
- ²³J.E. Hirsch, Phys. Rev. B **48**, 3327 (1993); **48**, 3340 (1993); **48**, 9815 (1993).
- ²⁴J.E. Hirsch and F. Marsiglio, Phys. Rev. B **43**, 424 (1991).
- ²⁵J.S. Schilling and S. Klotz, in *Physical Properties of High-Temperature Superconductors*, edited by D.M. Ginsberg (World Scientific, Singapore, 1992), Vol. 3.
- ²⁶F. Marsiglio and J.E. Hirsch, Phys. Rev. B **41**, 6435 (1990).
- ²⁷F. Marsiglio and J.E. Hirsch, Physica C **165**, 71 (1990).
- ²⁸D.K. Finnemore, J.E. Ostenson, S.L. Bud'ko, G. Lapertot, and P.C. Canfield, Phys. Rev. Lett. **86**, 2420 (2001).
- ²⁹S.L. Bud'ko, C. Petrovic, G. Lapertot, C.E. Cunningham, P.C. Canfield, M-H. Jung, and A.H. Lacerda, Phys. Rev. B **63**, 220503 (2001).
- ³⁰R.K. Kremer, B.J. Gibson, and K. Ahn, cond-mat/0102432 (unpublished).
- ³¹Furthermore, in the cuprates additional phenomena and complications arise due to the presence of antiferromagnetism nearby in the phase diagram, which we have argued to be irrelevant to the physics of superconductivity of these materials Ref. 12.
- ³²S. Uchida, K. Tamasaku, and S. Tajima, Phys. Rev. B **53**, 14 558 (1996); C. Panagopoulos *et al.*, *ibid.* **60**, 14 617 (1999).